JOURNAL OF COMPUTATIONAL PHYSICS 27, 410–427 (1978)

# Time-Dependent Solution of a Premixed Laminar Flame

STEPHEN B. MARGOLIS

*Applied Mathematics Division 8322, Sandia Laboratories, Livermore, California 94550*

Received May 12, 1977; revised August 8, 1977

The one-dimensional, time-dependent, multicomponent premixed laminar flame is solved via a highly accurate method of lines approach. The neglect of pressure variations and viscous dissipation and the use of a Lagrangian spatial coordinate reduce the problem to a system of parabolic partial differential equations for the species concentrations and the temperature. Introducing an appropriate B-spline (finite element) basis for the spatial variation and imposing collocation and boundary conditions on the time-dependent coefficients produce a stiff ordinary initial value problem which can be solved by standard techniques. Physical results of special interest include the transient and steady-state profiles of fluid velocity, temperature, and species concentrations through the reaction zone and the upstream velocity (flame speed) of the combustible mixture required to asymptotically stabilize the flame. The analysis is illustrated for the case of an ozone decomposition flame and a comparison with other theoretical predictions shows that the use of less accurate methods can result in significant errors in the predicted values of minor species profiles and the flame speed.

## 1. INTRODUCTION

Theoretical investigations of premixed laminar flames have essentially followed two different approaches. One formulation, first adopted by Hirschfelder *et al.* [1], seeks a solution to the time-independent equations and, for one-dimensional geometry, results in a two-point boundary value problem. It is also an eigenvalue problem due to the fact that the upstream fluid velocity (flame speed) required to stabilize the flame is an unknown quantity. Williams [2] summarizes various solution techniques for simple steady flames and Wilde [3] describes a general iterative technique based on a quasi-linearization method.

The second approach, first described by Spalding [4], treats the full time-dependent equations but does not require that the flame speed be known a priori. This description appears to be mathematically more straight-forward than the steady-state approach. Solution methods for general chemical-kinetic schemes have thus far been based on a discretization of the spatial coordinate using finite difference approximations (cf. Spalding *et al.* [5] and Bledjian [6]). The present work describes an alternative method of lines technique involving collocation with *B*-splines which is capable of providing highly accurate approximate solutions to the time-dependent equations. This high



0021-9991/78/0273-0410$02.00/0

order accuracy is desirable in order to provide reliable tests of proposed chemical reaction mechanisms and uncertain rate constants. A comparison of the results obtained here with other published results illustrates the errors which can occur when lower order methods are used.

## 2. Governing Equations

The physical problem is illustrated in Fig. 1. A premixed combustible fluid mixture emerges from a flat flame burner, passes through a reaction zone in which chemical changes take place, and emerges in a burned state. The relevant variables of interest here are the mass fractions $Y^{(k)}$, $k = 1,..., N$, temperature $T$, density $\rho$, and velocity $u$

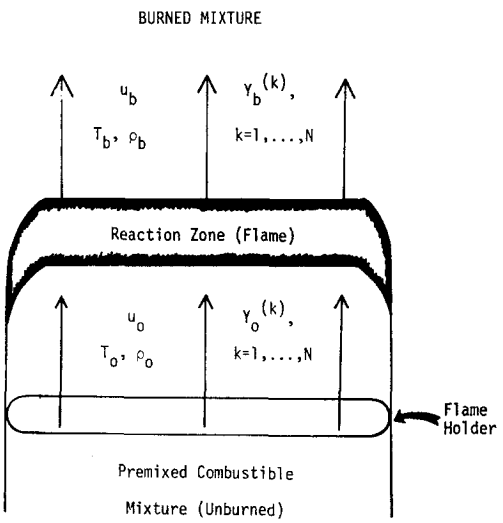


FIG. 1. A premixed laminar flat flame.

of the fluid. The goal is to be able to theoretically predict these quantities as functions of space and time. To simplify the model, the flow is assumed to be one-dimensional, the presence of the flame holder is ignored, and forced convection effects are assumed to dominate any natural convection effects due to gravity (i.e., the body force is neglected). The conservation equations describing the model are then overall continuity

$$\frac{\partial \rho}{\partial t} + \frac{\partial (\rho u)}{\partial x} = 0, \tag{2.1}$$

conservation of momentum

$$\rho \frac{\partial u}{\partial t} + \rho u \frac{\partial u}{\partial x} = -\frac{\partial p}{\partial x} + \frac{\partial}{\partial x}\left[\left(\kappa + \frac{4}{3}\mu\right)\frac{\partial u}{\partial x}\right], \tag{2.2}$$

conservation of species

$$\rho \frac{\partial Y^{(k)}}{\partial t} + \rho u \frac{\partial Y^{(k)}}{\partial x} = R_k M_k + \frac{\partial}{\partial x}\left(\rho D_k \frac{\partial Y^{(k)}}{\partial x}\right), \tag{2.3}$$

$$k = 1,..., N = \text{no. of species},$$

and conservation of energy

$$\rho c_p \frac{\partial T}{\partial t} + \rho c_p u \frac{\partial T}{\partial x} = \frac{\partial p}{\partial t} + u \frac{\partial p}{\partial x} + \left(\kappa + \frac{4}{3}\mu\right)\left(\frac{\partial u}{\partial x}\right)^2 + \frac{\partial}{\partial x}\left(\lambda \frac{\partial T}{\partial x}\right) - \sum_{k=1}^{N} R_k M_k h^{(k)} + \sum_{k=1}^{N} \rho D_k c_p^{(k)} \frac{\partial Y^{(k)}}{\partial x} \frac{\partial T}{\partial x}. \tag{2.4}$$

In these equations, a Fick's law is assumed to govern the diffusion of each species and the effects of radiative heat transfer and thermal and pressure diffusion have been neglected. The variables appearing in these equations have their usual meanings and

TABLE I

Definitions of Variables

| Symbol | Definition |
|---|---|
| $x$ | Space coordinate |
| $t$ | Time coordinate |
| $\rho$ | Density of fluid mixture |
| $\rho^{(k)}$ | Density of $k$th species |
| $Y^{(k)}$ | Mass fraction of $k$th species ($=\rho^{(k)}/\rho$) |
| $u$ | Velocity of fluid mixture |
| $R$ | Universal gas constant |
| $p$ | Hydrostatic pressure |
| $\mu$ | First (shear) viscosity coefficient |
| $\kappa$ | Second (bulk) viscosity coefficient |
| $R_k$ | Rate of production of $k$th species by chemical reactions (moles/vol-sec) |
| $M_k$ | Molecular weight of $k$th species |
| $D_k$ | Binary diffusion coefficient for the $k$th species into the mixture of remaining species |
| $c_p$ | Specific heat capacity at constant pressure of the fluid mixture |
| $c_p^{(k)}$ | Specific heat capacity at constant pressure of the $k$th species |
| $T$ | Temperature of the fluid |
| $\lambda$ | Thermal conductivity of the fluid mixture |
| $h_0^{(k)}$ | Standard molal enthalpy of formation of $k$th species at temperature $T_0$ |
| $h^{(k)}$ | Specific enthalpy of $k$th species $[=M_k^{-1}h_0^{(k)} + \int_{T_0}^{T} c_p^{(k)}(\bar{T})\, d\bar{T}]$ |

are summarized in Table I. The system of Eqs. (2.1)–(2.4) is closed by adding the equation of state (assumed to be that of an ideal gas)

$$p = \rho \sum_{k=1}^{N} \frac{Y^{(k)}}{M_k} RT. \tag{2.5}$$

In order to simplify these equations, the effects of viscosity are assumed to be negligible and fluid velocities are assumed to be small compared to the speed of sound. This last approximation, valid for weak deflagrations (cf. Williams [2]), allows one to integrate Eq. (2.2) and obtain the condition

$$p \approx p_0 = \text{const.} \tag{2.6}$$

The simplified set of equations is then

$$\frac{\partial \rho}{\partial t} + \frac{\partial (\rho u)}{\partial x} = 0, \tag{2.7}$$

$$\frac{\partial Y^{(k)}}{\partial t} + u \frac{\partial Y^{(k)}}{\partial x} = \frac{1}{\rho} R_k M_k + \frac{1}{\rho} \frac{\partial}{\partial x} \left( \rho D_k \frac{\partial Y^{(k)}}{\partial x} \right), \qquad k = 1,..., N, \tag{2.8}$$

$$\frac{\partial T}{\partial t} + u \frac{\partial T}{\partial x} = -\frac{1}{\rho c_p} \sum_{k=1}^{N} R_k M_k h^{(k)} + \frac{1}{\rho c_p} \frac{\partial}{\partial x} \left( \lambda \frac{\partial T}{\partial x} \right) + \sum_{k=1}^{N} \frac{c_p^{(k)}}{c_p} D_k \frac{\partial Y^{(k)}}{\partial x} \frac{\partial T}{\partial x}, \tag{2.9}$$

$$\rho = p_0 \Big/ \left( \sum_{k=1}^{N} \frac{Y^{(k)}}{M_k} RT \right). \tag{2.10}$$

The solution of Eqs. (2.7)–(2.10) is greatly facilitated by introducing a Lagrangian coordinate $\psi$ (cf. Spalding [4]),

$$\psi(x, t) = \int_0^x \rho(\bar{x}, t)\, d\bar{x}. \tag{2.11}$$

Since

$$\frac{\partial \psi}{\partial x} = \rho, \tag{2.12}$$

$$\frac{\partial \psi}{\partial t} = \int_0^x \frac{\partial \rho(\bar{x}, t)}{\partial t} d\bar{x} = -\int_0^x \frac{\partial}{\partial \bar{x}} (\rho u)\, d\bar{x} = -\rho u + m_0(t), \tag{2.13}$$

where

$$m_0(t) = \rho u \,|_{x=0}, \tag{2.14}$$

the continuity equation (2.7) is identically satisfied when $\psi$ and $t$ are used as independent variables. Using the relations

$$\frac{\partial}{\partial x} \to \frac{\partial \psi}{\partial x}\frac{\partial}{\partial \psi} = \rho \frac{\partial}{\partial \psi}, \tag{2.15}$$

$$\frac{\partial}{\partial t} \to \frac{\partial \psi}{\partial t}\frac{\partial}{\partial \psi} + \frac{\partial}{\partial t} = (-\rho u + m_0)\frac{\partial}{\partial \psi} + \frac{\partial}{\partial t}, \tag{2.16}$$

the remaining equations become

$$\frac{\partial Y^{(k)}}{\partial t} + m_0 \frac{\partial Y^{(k)}}{\partial \psi} = \frac{\partial}{\partial \psi}\left(\rho^2 D_k \frac{\partial Y^{(k)}}{\partial \psi}\right) + \frac{1}{\rho} R_k M_k, \qquad k = 1,..., N, \tag{2.17}$$

$$\frac{\partial T}{\partial t} + m_0 \frac{\partial T}{\partial \psi} = \frac{1}{c_p}\frac{\partial}{\partial \psi}\left(\rho\lambda \frac{\partial T}{\partial \psi}\right) - \frac{1}{\rho c_p}\sum_{k=1}^{N} R_k M_k h^{(k)} + \sum_{k=1}^{N} \frac{c_p^{(k)}}{c_p} \rho^2 D_k \frac{\partial Y^{(k)}}{\partial \psi}\frac{\partial T}{\partial \psi}, \tag{2.18}$$

where $\rho$, $R_k$, and $h_k$ are specified functions of the dependent variables $T$, $Y^{(1)},..., Y^{(N)}$. In practice, the variable $Y^{(N)}$ is usually eliminated by use of the relation

$$\sum_{k=1}^{N} Y^{(k)} = 1 \tag{2.19}$$

In order to completely determine the solution to the parabolic system of equations (2.17) and (2.18), one must specify initial and boundary conditions. These are most easily applied in a frame of reference in which the fluid is initially at rest. If the initial conditions are symmetric about $x = 0$, only the half line $0 \leqslant x < \infty$ need be considered and the boundary conditions are

$$\frac{\partial T}{\partial \psi} = \frac{\partial Y^{(1)}}{\partial \psi} = \cdots = \frac{\partial Y^{(N)}}{\partial \psi} = 0 \qquad \text{at} \quad \psi = 0, \infty \quad \text{for} \quad t \geqslant 0. \tag{2.20}$$

[Equation (2.11) is a strictly monotonic mapping from $0 \leqslant x < \infty$ onto $0 \leqslant \psi < \infty$.] These conditions correspond to zero flux of species and heat at the origin (due to symmetry) and at infinity. One also has that $u(x = 0, t) = 0$ for all $t$ so that the terms containing $m_0$ in Eqs. (2.17) and (2.18) vanish. The initial conditions (in the $\psi$ coordinate) are

$$T(\psi, t = 0) = T_0(\psi), \tag{2.21}$$

$$Y^{(k)}(\psi, t = 0) = Y_0^{(k)}(\psi), \qquad k = 1,..., N, \tag{2.22}$$

for $0 \leqslant \psi < \infty$.

Once Eqs. (2.17)–(2.22) have been solved for $T$, $\rho$, $Y^{(1)},\ldots, Y^{(N)}$ as functions of $\psi$ and $t$, Eq. (2.12) can be integrated to give

$$x(\psi, t) = \int_0^{\psi} \frac{1}{\rho(\bar{\psi}, t)}\, d\bar{\psi}, \tag{2.23}$$

which in turn can be used to obtain $T$, $\rho$, $Y^{(1)},\ldots, Y^{(N)}$ as implicit functions of $x$ and $t$. The fluid velocity, from Eqs. (2.11) and (2.13), is then

$$u(x, t) = -\frac{1}{\rho(x, t)} \int_0^{x} \frac{\partial \rho(\bar{x}, t)}{\partial t}\, d\bar{x}. \tag{2.24}$$

## 3. Method of Solution

It is convenient to first nondimensionalize Eqs. (2.17) and (2.18). Hence, the following nondimensional variables are introduced:

$$\rho^* \equiv \rho/\rho_\infty\,, \qquad T^* \equiv T/T_\infty\,; \tag{3.1a, b}$$

$$D^*_k \equiv D_k/D_\infty\,, \qquad \lambda^* \equiv \lambda/\lambda_\infty\,; \tag{3.2a, b}$$

$$c^*_p \equiv c_p/c_{p_\infty}\,, \qquad c_p^{(k)*} \equiv c_p^{(k)}/c_{p_\infty} \tag{3.3a, b}$$

$$h^* \equiv h/c_{p_\infty}T_\infty\,, \qquad M^*_k \equiv M_k/M_\infty\,; \tag{3.4a, b}$$

$$t^* \equiv t/t_\infty\,, \qquad R^*_k \equiv R_k M_\infty t_\infty/\rho_\infty\,; \tag{3.5a, b}$$

$$x^* \equiv x/l_\infty\,, \qquad l_\infty = (\lambda_\infty t_\infty/\rho_\infty c_{p_\infty})^{1/2}; \tag{3.6}$$

$$\psi^* \equiv \psi/\psi_\infty\,, \qquad \psi_\infty = \rho_\infty l_\infty = (\rho_\infty \lambda_\infty t_\infty/c_{p_\infty})^{1/2}. \tag{3.7}$$

Here, $\rho_\infty$, $T_\infty$, $D_\infty$, $\lambda_\infty$, $c_{p_\infty}$, and $M_\infty$ represent characteristic values of density, temperature, mass diffusivity, heat conductivity, specific heat capacity, and molecular weight, respectively. The characteristic time $t_\infty$ is based on a "significant" chemical time scale (there are in general a number of such scales due to the fact that there is wide variation among the rates at which the different chemical reactions occur; the differential equations are therefore "stiff"). The characteristic length $l_\infty$ is a diffusion length scale based on $t_\infty$ (there is no natural length scale in the problem). Substituting this scaling into Eqs. (2.17) and (2.18) leads to

$$\frac{\partial Y^{(k)}}{\partial t^*} = (Le_\infty)^{-1} \frac{\partial}{\partial \psi^*}\left(\rho^{*2} D^*_k \frac{\partial Y^{(k)}}{\partial \psi^*}\right) + \frac{1}{\rho^*} R^*_k M^*_k\,, \qquad k = 1,\ldots, N, \tag{3.8}$$

$$\frac{\partial T^*}{\partial t^*} = \frac{1}{c^*_p} \frac{\partial}{\partial \psi^*}\left(\rho^* \lambda^* \frac{\partial T^*}{\partial \psi^*}\right) - \frac{1}{\rho^* c^*_p} \sum_{k=1}^{N} R^*_k M^*_k h^{(k)*}$$

$$+ (Le_\infty)^{-1} \sum_{k=1}^{N} \frac{c_p^{(k)*}}{c^*_p} \rho^{*2} D^*_k \frac{\partial Y^{(k)}}{\partial \psi^*} \frac{\partial T}{\partial \psi^*}\,, \tag{3.9}$$

where

$$Le_\infty = \lambda_\infty/\rho_\infty D_\infty c_{p_\infty} \tag{3.10}$$

is a characteristic Lewis number.

The method of lines technique adopted here is based on a collocation procedure (cf. [7]). It is assumed that the solution can be written in the form

$$\begin{bmatrix} Y^{(1)} \\ Y^{(2)} \\ \vdots \\ Y^{(N)} \\ T^* \end{bmatrix} \cong \sum_{i=1}^{m} \begin{bmatrix} C_1^{(i)}(t^*) \\ C_2^{(i)}(t^*) \\ \vdots \\ C_N^{(i)}(t^*) \\ C_{N+1}^{(i)}(t^*) \end{bmatrix} F_i(\psi^*), \tag{3.11}$$

where the collection of functions $F_i(\psi^*)$, $i = 1,..., m$, span the solution space for any fixed $t^*$ to within a small error tolerance $\epsilon_1$. It is also assumed that the truncation error, the amount by which the approximate solution (3.11) fails to solve the partial differential equations (3.8) and (3.9), is at most a small value $\epsilon_2$. The time-dependent coefficients $C_1^{(i)}$, $C_2^{(i)}$,..., $C_{N+1}^{(i)}$, $i = 1,..., m$, are uniquely determined by requiring that Equation (3.11) satisfy the two boundary conditions in Eq. (2.20) and that it satisfy Eqs. (3.8) and (3.9) exactly at $m - 2$ interior (collocation) points $\psi^*_1$, $\psi^*_2$,..., $\psi^*_{m-2}$. This results in a system of coupled nonlinear ordinary differential equations for these coefficients which may be numerically integrated by standard techniques. The initial values for the coefficients are obtained by requiring Eq. (3.11) to satisfy the initial conditions in Eqs.(2.21) and (2.22) at $m$ (interpolation) points (including the two boundary points).

The particular functions $F_i(\psi^*)$ used in this paper belong to a special class of piecewise polynomials called $B$-splines. The $i$th normalized $B$-spline of order $k$, $N_{i,k}(z)$, is a function of $z$ and defined by a subset of points ($\equiv$knots)$\{s_j\}_{j=i}^{i+k}$ (cf. Curry and Schoenberg [8], de Boor [9]). The $B$-spline $N_{i,k}(z)$ is zero outside the interval $s_i \leqslant z \leqslant s_{i+k}$, non-negative at $z = s_i$ and $z = s_{i+k}$, and strictly positive for $s_i < z < s_{i+k}$. This desirable property means that the system of ordinary equations for the coefficients $\{C_1^{(i)},..., C_{N+1}^{(i)}\}_{i=1}^m$ will not be fully coupled due to the fact that at any collocation point, at most $k$ of the $B$-spline functions are non-zero. In any interval such that $s_i \leqslant s_j < z < s_{j+1} \leqslant s_{i+k}$, $N_{i,k}(z)$ is a polynomial of order $k$ (degree $k - 1$). If $s_l$, $s_i \leqslant s_l \leqslant s_{i+k}$, is a knot of multiplicity $k - \nu$, then $d^\nu N_{i,k}/dz^\nu$ is discontinuous at $z = s_l$ and all lower order derivatives are continuous at $z = s_l$. For the special case of equally spaced knots $s_j = s_i + (j - 1)h$, $j = 1,..., k + 1$, $h > 0$, $N_{i,k}(z)$ is a bell-shaped function symmetric about $z = s_i + \frac{1}{2}kh$.

The motivation for generating $B$-splines is contained in the $B$-spline representation theorem of Curry and Schoenberg [8]. Consider the linear space of functions $\mathscr{P}_{k,\xi,\nu}$, $\xi = \{\xi_i\}_{i=1}^{l+1}$, $\nu = \{\nu_i\}_{i=2}^{l}$, consisting of the set of all piecewise functions $f(z)$ which are polynomials of order $k$ in each interval $\xi_j \leqslant z < \xi_{j+1}$, $j = 1,..., l$, and which obey the continuity conditions

$$\left.\frac{d^{j-1}f}{dz^{j-1}}\right|_{z=\xi_i^+} - \left.\frac{d^{j-1}f}{dz^{j-1}}\right|_{z=\xi_i^-} = 0, \qquad j = 1,..., \nu_i\,; \quad i = 2,..., l. \tag{3.12}$$

The dimension of the space $\mathscr{P}_{k,\xi,\nu}$ is $m$,

$$m = kl - \sum_{i=2}^{l} \nu_i \tag{3.13}$$

(de Boor [10]) and the theorem specifies the construction of a knot sequence $\{s_i\}_{i=1}^{m+k}$ such that the sequence $\{N_{i,k}\}_{i=1}^{m}$ of $B$-splines of order $k$ is a basis for $\mathscr{P}_{k,\xi,\nu}$ on the interval $[s_k\,, s_{m+1}]$. As a consequence of this theorem, one has the approximation property (Swartz and Varga [11]) that for a general (breakpoint) sequence $\xi$ and a sufficiently smooth function $w(z)$,

$$\frac{d^j w(z)}{dz^j} = \sum_{i=1}^{m} \alpha_i \frac{d^j N_{i,k}(z)}{dz^j} + O(h^{k-j}), \tag{3.14}$$

where the $\alpha_i$'s are constants and

$$h = \max_i (\xi_{i+1} - \xi_i). \tag{3.15}$$

Thus, the tolerance $\epsilon_1$ and the truncation error $\epsilon_2$ of the preceding section are $O(h^k)$ and $O(h^{k-2})$, respectively.

## 4. Example: Ozone Decomposition

The applicability of the above analysis was demonstrated by calculating the structure of an ozone decomposition flame. In order to compare the results with other theoretical predictions, the following nonessential approximations were made in the fluid conservation equations (cf. Bledjian [6]):

$$D_1 = D_2 = \cdots = D_N \equiv D \text{ and } \rho^2 D = \text{const} = \rho_\infty{}^2 D_\infty\,, \tag{4.1}$$

$$\rho\lambda = \text{const} = \rho_\infty \lambda_\infty\,, \tag{4.2}$$

$$c_p^{(1)} = c_p^{(2)} = \cdots = c_p^{(N)} \equiv c_p = \text{const} = c_{p_\infty}\,. \tag{4.3}$$

The ozone decomposition mechanism is

$$O_3 + \bar{X} \underset{k_1{}^b}{\overset{k_1{}^f}{\rightleftarrows}} O_2 + O + \bar{X}, \tag{4.4}$$

$$O + O_3 \underset{k_4{}^b}{\overset{k_4{}^f}{\rightleftarrows}} 2O_2\,, \tag{4.5}$$

$$O_2 + \bar{X} \underset{k_5{}^b}{\overset{k_5{}^f}{\rightleftarrows}} 2O + \bar{X}, \tag{4.6}$$

where $\underline{X}$ represents any of the three species $O$, $O_2$, $O_3$ (hence there are seven reversible reactions which can occur).

The rate of production $R_k$ of the $k$th species appearing in Eqs. (2.17) and (2.18) is given by the law of mass action

$$R_k = \sum_{m=1}^{M} (\nu''_{k,m} - \nu'_{k,m}) \left[ k_m{}^f \prod_{n=1}^{N} c_n^{\nu'_{n,m}} - k_m{}^b \prod_{n=1}^{N} c_n^{\nu''_{n,m}} \right], \tag{4.7}$$

where $\nu'_{k,m}(\nu''_{k,m})$ is the stoichiometric coefficient of species $k$, $k = 1,..., N$, appearing as a reactant (product) in the reversible reaction $m$, $m = 1,..., M$. The variable $c_n$ is the *mole* concentration of species $n$ and is related to the mass fraction $Y^{(n)}$ by

$$c_n = (\rho/M_n)\, Y^{(n)}. \tag{4.8}$$

The function $k_m{}^f(k_m{}^b)$ is the so-called specific rate constant for the forward (backward) mode of reaction $m$ and is usually given by the semi-empirical Arrhenius expression

$$k_m{}^f = B_m{}^f T^{s_m{}^f} e^{-E_m{}^f/RT}, \qquad B_m{}^f,\ s_m{}^f,\ E_m{}^f = \text{const}, \tag{4.9}$$

with a similar expression for $k_m{}^b$. The constant $E_m{}^f(E_m{}^b)$ is the activation energy of the forward (backward) mode of reaction $m$.

Utilizing Eqs. (4.1)–(4.3) and (4.7)–(4.9), the nondimensionalized equations (3.8) and (3.9) become

$$\frac{\partial}{\partial t^*} \begin{bmatrix} Y^{(1)} \\ Y^{(2)} \\ Y^{(3)} \\ T^* \end{bmatrix} = \begin{bmatrix} Le_\infty^{-1} & & & 0 \\ & Le_\infty^{-1} & & \\ & & Le_\infty^{-1} & \\ 0 & & & 1 \end{bmatrix} \frac{\partial^2}{\partial \psi^{*2}} \begin{bmatrix} Y^{(1)} \\ Y^{(2)} \\ Y^{(3)} \\ T^* \end{bmatrix} + \begin{bmatrix} P^{(1)}(Y^{(1)}, Y^{(2)}, Y^{(3)}, T^*) \\ P^{(2)}(Y^{(1)}, Y^{(2)}, Y^{(3)}, T^*) \\ P^{(3)}(Y^{(1)}, Y^{(2)}, Y^{(3)}, T^*) \\ Q(Y^{(1)}, Y^{(2)}, Y^{(3)}, T^*) \end{bmatrix}, \tag{4.10}$$

$$\begin{aligned} T^*(\psi^*, t^* = 0) &= T_0(\psi^*), \\ Y^{(k)}(\psi^*, t^* = 0) &= Y_0^{(k)}(\psi^*), \qquad k = 1, 2, 3, \end{aligned} \tag{4.11}$$

$$\frac{\partial T^*}{\partial \psi^*} = \frac{\partial Y^{(1)}}{\partial \psi^*} = \frac{\partial Y^{(2)}}{\partial \psi^*} = \frac{\partial Y^{(3)}}{\partial \psi^*} = 0 \qquad \text{at} \quad \psi^* = 0, \infty \quad \text{for} \quad t^* \geqslant 0. \tag{4.12}$$

The variables $Y^{(1)}$, $Y^{(2)}$, $Y^{(3)}$ here denote the mass fractions of O, $O_2$, and $O_3$, respectively. The nondimensional production terms $Q$ and $P^{(k)}$, $k = 1, 2, 3$, are

$$P^{(k)} = \sum_{m=1}^{M=7} M_k{}^* (\nu''_{k,m} - \nu'_{k,m}) \left[ (k_m{}^f)^* \rho^{*\alpha_m - 1} \prod_{n=1}^{N=3} \left\{ \frac{Y^{(n)}}{M^*{}_n} \right\}^{\nu'_{n,m}} \right.$$

$$\left. - (k_m{}^b)^* \rho^{*\beta_m - 1} \prod_{n=1}^{N=3} \left\{ \frac{Y^{(n)}}{M^*{}_n} \right\}^{\nu''_{n,m}} \right] \tag{4.13}$$

and

$$Q = -\sum_{m=1}^{M=7} h_r^{(m)*}\left[(k_m{}^f)^*\,\rho^{*\alpha_m-1}\prod_{n=1}^{N=3}\left\{\frac{Y^{(n)}}{M^*{}_n}\right\}^{\nu'_{n,m}}\right.$$

$$\left. -\,(k_m{}^b)^*\,\rho^{*\beta_m-1}\prod_{n=1}^{N=3}\left\{\frac{Y^{(n)}}{M^*{}_n}\right\}^{\nu''_{n,m}}\right], \tag{4.14}$$

where

$$\alpha_m \equiv \sum_{n=1}^{N=3}\nu'_{n,m}\,; \qquad \beta_m \equiv \sum_{n=1}^{N=3}\nu''_{n,m}\,, \tag{4.15}$$

$$(k_m{}^f)^* \equiv k_m{}^f t_\infty \left(\frac{\rho_\infty}{M_\infty}\right)^{\alpha_m-1}, \tag{4.16}$$

$$(k_m{}^b)^* \equiv k_m{}^b t_\infty \left(\frac{\rho_\infty}{M_\infty}\right)^{\beta_m-1}. \tag{4.17}$$

The number

$$h_r^{(m)*} \equiv \sum_{k=1}^{N=3}\frac{h_0^{(k)}}{M_\infty c_{p_\infty} T_\infty}(\nu''_{k,m} - \nu'_{k,m}) \tag{4.18}$$

is the nondimensional enthalpy of reaction for the $m$th reaction ($h_0^{(k)}$ is the molal enthalpy of formation of the $k$th species). The thermodynamics and kinetics data used were the same as those used by Bledjian [6] and Hirschfelder *et al.* [1] and are given in Table II. The characteristic time $t_\infty$ was chosen on the basis of the forward reaction (4.4) since this is the reaction which must occur (for the case of a combustible mixture of $O_2$ and $O_3$) before a flame can develop and propagate. Specifically, $t_\infty$ was taken to be that value which made $(k_1{}^f)^*$ in Eq. (4.16) equal to unity for $T^* = 2.5$.

The initial conditions on the mass fractions and temperature were taken to be

$$Y_0^{(1)}(\psi^*) = \begin{cases} 0.0005\cos^5[(\pi/2)(\psi^*/1.2)^7], & 0 \leqslant \psi^* \leqslant 1.2, \\ 0, \qquad \psi^* > 1.2, \end{cases} \tag{4.19}$$

$$Y_0^{(2)}(\psi^*) = \begin{cases} \frac{2}{3} + (\frac{1}{3} - 0.0005)\cos^5[(\pi/2)(\psi^*/1.2)^7], & 0 \leqslant \psi^* \leqslant 1.2, \\ \frac{2}{3}, \qquad \psi^* > 1.2, \end{cases} \tag{4.20}$$

$$Y_0^{(3)}(\psi^*) = 1 - Y_0^{(1)} - Y_0^{(2)}$$

$$= \begin{cases} \frac{1}{3} - \frac{1}{3}\cos^5[(\pi/2)(\psi^*/1.2)^7], & 0 \leqslant \psi^* \leqslant 1.2, \\ \frac{1}{3}, \qquad \psi^* > 1.2, \end{cases} \tag{4.21}$$

$$T_0{}^*(\psi^*) = \begin{cases} 1.0 + 3.166667\cos^5[(\pi/2)(\psi^*/1.2)^7], & 0 \leqslant \psi^* \leqslant 1.2, \\ 1.0, \qquad \psi^* > 1.2. \end{cases} \tag{4.22}$$

These initial conditions correspond to a pocket of burned or nearly burned gas at the origin surrounded by a combustible mixture of 75 % $O_2$ and 25 % $O_3$ (by volume) at a

TABLE II

Data for Ozone Decomposition

| Symbol | Value | Symbol | Value |
|---|---|---|---|
| $E_1^f, E_2^f, E_3^f$ | 24140 cal/mole | $B_4^b$ | $1.88 \times 10^6$ |
| $E_4^f$ | 6000 cal/mole | $B_5^b, B_6^b, B_7^b$ | $2.47 \times 10^2$ |
| $E_5^f, E_6^f, E_7^f$ | 117350 cal/mole | $h_0^{(1)}$ | 58675 cal/mole |
| $E_1^b, E_2^b, E_3^b$ | 0 | $h_0^{(2)}$ | 0 |
| $E_4^b$ | 99210 cal/mole | $h_0^{(3)}$ | 34535 cal/mole |
| $E_5^b, E_6^b, E_7^b$ | 0 | $\rho_\infty$ | $1.201 \times 10^{-3}$ g/cm$^3$ |
| $s_1^f, s_2^f, s_3^f$ | 5/2 | $T_\infty$ | 300 °K |
| $s_4^f$ | 5/2 | $c_{p_\infty}$ | 0.2524 cal/g-°K |
| $s_5^f, s_6^f, s_7^f$ | 5/2 | $\lambda_\infty$ | $9.112 \times 10^{-5}$ cal/cm-sec-°K |
| $s_1^b, s_2^b, s_3^b$ | 7/2 | $D_\infty$ | $\lambda_\infty/\rho_\infty c_{p_\infty}$ Le$_\infty$ |
| $s_4^b$ | 5/2 | $M_\infty$ | 16 g/mole |
| $s_5^b, s_6^b, s_7^b$ | 7/2 | $l_\infty$ | $4.203 \times 10^{-3}$ cm |
| $B_1^f, B_2^f, B_3^f$ | $6.76 \times 10^6$ | $t_\infty$ | $5.878 \times 10^{-5}$ sec |
| $B_4^f$ | $4.58 \times 10^6$ | $l_\infty/t_\infty$ | 71.51 cm/sec |
| $B_5^f, B_6^f, B_7^f$ | $5.71 \times 10^6$ | $p_0$ | 0.821 atm. |
| $B_1^b, B_2^b, B_3^b$ | $1.18 \times 10^2$ | $M_1$ | 16 g/mole |
| | | $M_2$ | 32 g/mole |
| | | $M_3$ | 48 g/mole |

temperature of 300°K (the pressure was taken to be 0.821 atm.), which is identical to the mixture used in [1, 6]. The quasi-steady flame structure and propagation velocity are independent of the initial profiles near the origin, but it was found that the approach to a quasi-steady state was most rapid when their values near $\psi^* = 0$ were approximately those of the burned mixture. In the actual integration of the equations by the method described above, use was made of the subroutine package PDECOL of Madsen and Sincovec [12]. This code, which is applicable to general systems of partial differential equations of the form $\mathbf{u}_t = f(x, t, \mathbf{u}, \mathbf{u}_x, \mathbf{u}_{xx})$, combines the $B$-spline subroutines of De Boor [10] with a state of the art version of a stiff ordinary differential equation integrator (Hindmarsh [13]).

The boundary condition at infinity was applied at $\psi^* = 50$, a value large enough to allow the full development of the flame before any effects could be felt there. Rather than use the boundary conditions [Eq. (4.12)] to eliminate some of the time-dependent coefficients in Eq. (3.11), these conditions were differentiated with respect to $t^*$ to form additional differential equations for these coefficients:

$$\frac{\partial^2}{\partial t^* \partial \psi^*} \begin{bmatrix} Y^{(1)} \\ Y^{(2)} \\ Y^{(3)} \\ T^* \end{bmatrix} = 0 \qquad \text{at} \quad \psi^* = 0, \infty \quad \text{for} \quad t^* \geqslant 0. \tag{4.23}$$

Since initial conditions on the $C_j^{(i)}(t^*)$, $i = 1,..., m$, $j = 1,..., N + 1 = 4$, were obtained from interpolation conditions on the dependent variables, a sufficient number of breakpoints were used near $\psi^* = 0$ to insure that initial values of their derivatives were nearly zero.

The maximum breakpoint spacing was 0.2, the order of the $B$-splines was 6, and the continuity conditions at the breakpoints were that the $B$-splines and their first 4 derivatives be continuous at the breakpoints. The spatial truncation error was thus fourth order and the error tolerance on the time integration of the $C_j^{(i)}(t^*)$ was chosen to be sufficiently small so that no larger errors were generated by the ordinary differential equation integrator. $A$ total of 270 breakpoints were used, resulting in $m - 2 = 272$ collocation points for a system of three partial differential equations [the relation (2.19) was used to eliminate one of the mass fraction variables]. Including the boundary equations (4.23), the use of (3.11) and (2.19) in (4.10) gave a total of $3m = 822$ coupled ordinary differential equations.

## 5. Discussion of Results

The time development for $Le_\infty = 1$ of the right propagating flame (the profiles are symmetric with respect to the origin) from the initial conditions [Eqs. (4.19)–(4.22)] is shown in the Lagrangian coordinate $\psi^*$ in Figs. 2a–h. Figures 3a–h show the development in the physical coordinate $x^*$. These pictures, taken in sequence, illustrate the early diffusion of heat and individual species, the ignition process, and the final approach to a steadily propagating flame front. In these figures, one unit in time is $t_\infty = 5.878 \times 10^{-5}$ sec, one unit in the Lagrangian coordinate is $\rho_\infty l_\infty = 5.048 \times 10^{-6}$ g/cm$^2$, and one unit in the physical coordinate is $l_\infty = 4.203 \times 10^{-3}$ cm. The picture at $t^* = 35$, obtained after about 20 minutes of CDC 6600 computer time, is the quasi-steady profile of a fully developed ozone flame.

A comparison of these results with those of Bledjian [6], who used a lower order finite difference method, shows a significant difference in the profile of $Y^{(1)}$ (atomic oxygen). In particular, the results here support those of Hirschfelder *et al.* [1], who also obtained a sharp gradient of $Y^{(1)}$ (with respect to temperature) at the hot boundary using a time-independent approach. This result is not surprising in view of the multiple time scales, for a consideration of the rates at which each of the reactions [Eqs. (4.4)–(4.6)] occurs shows that the flame structure and propagation velocity is dominated by the decay of $O_3$ into $O_2$ and O and the recombination of O with $O_3$ to form $O_2$. Due primarily to the small concentrations of O, the recombination of O with itself to form $O_2$ only becomes significant (compared to the other reactions) after the mixture is nearly burned and is thus responsible for the relatively slow decay (in time) of the mass fraction of O from its maximum value of approximately $4.51 \times 10^{-3}$ just behind the flame.

A plot of the fluid velocity (made dimensionless by $l_\infty/t_\infty = 71.51$ cm/sec) for a fully developed flame, obtained from an accurate numerical approximation to the

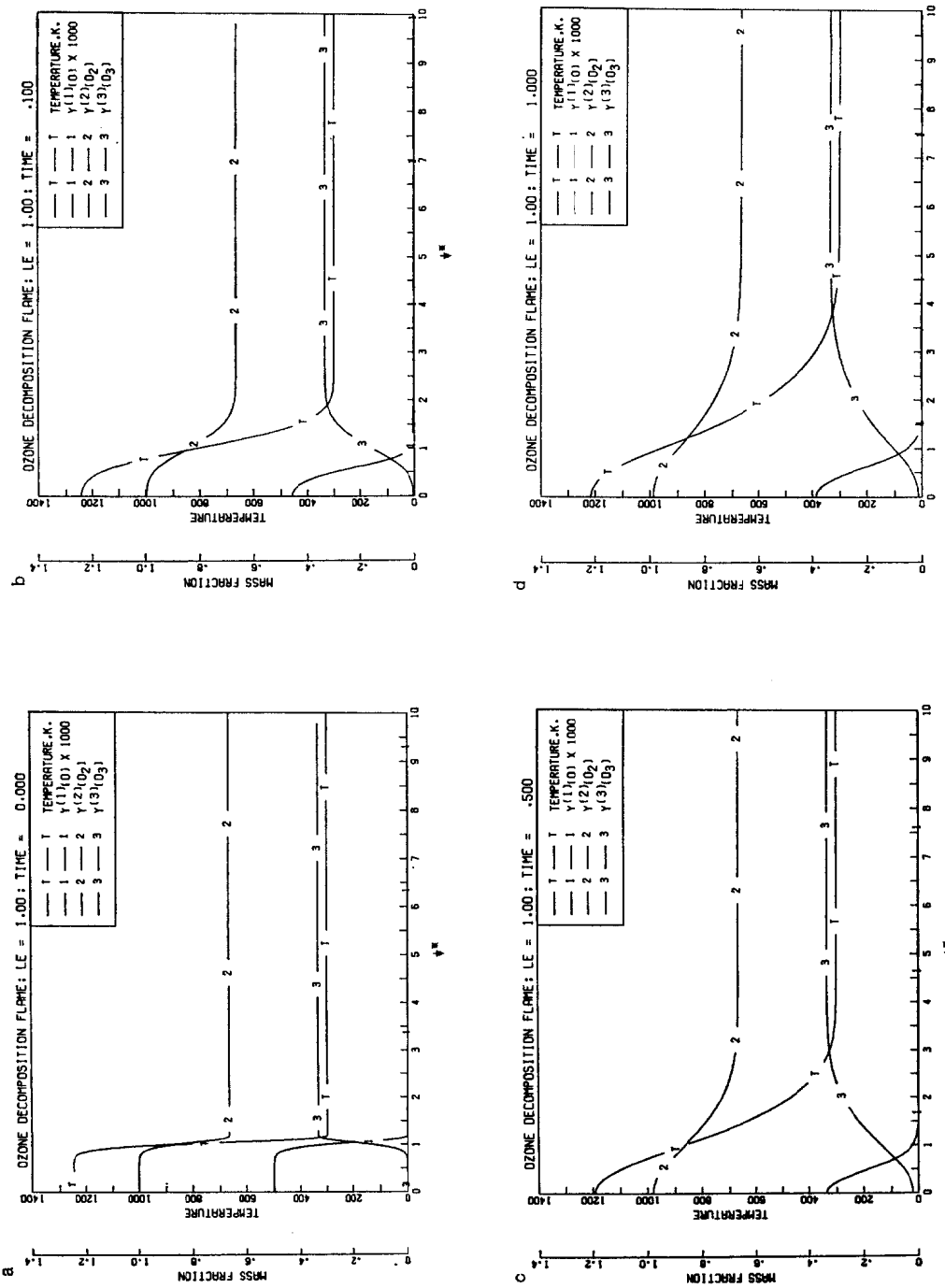


FIG. 2. Time development in the Lagrangian coordinate of an ozone decomposition flame.

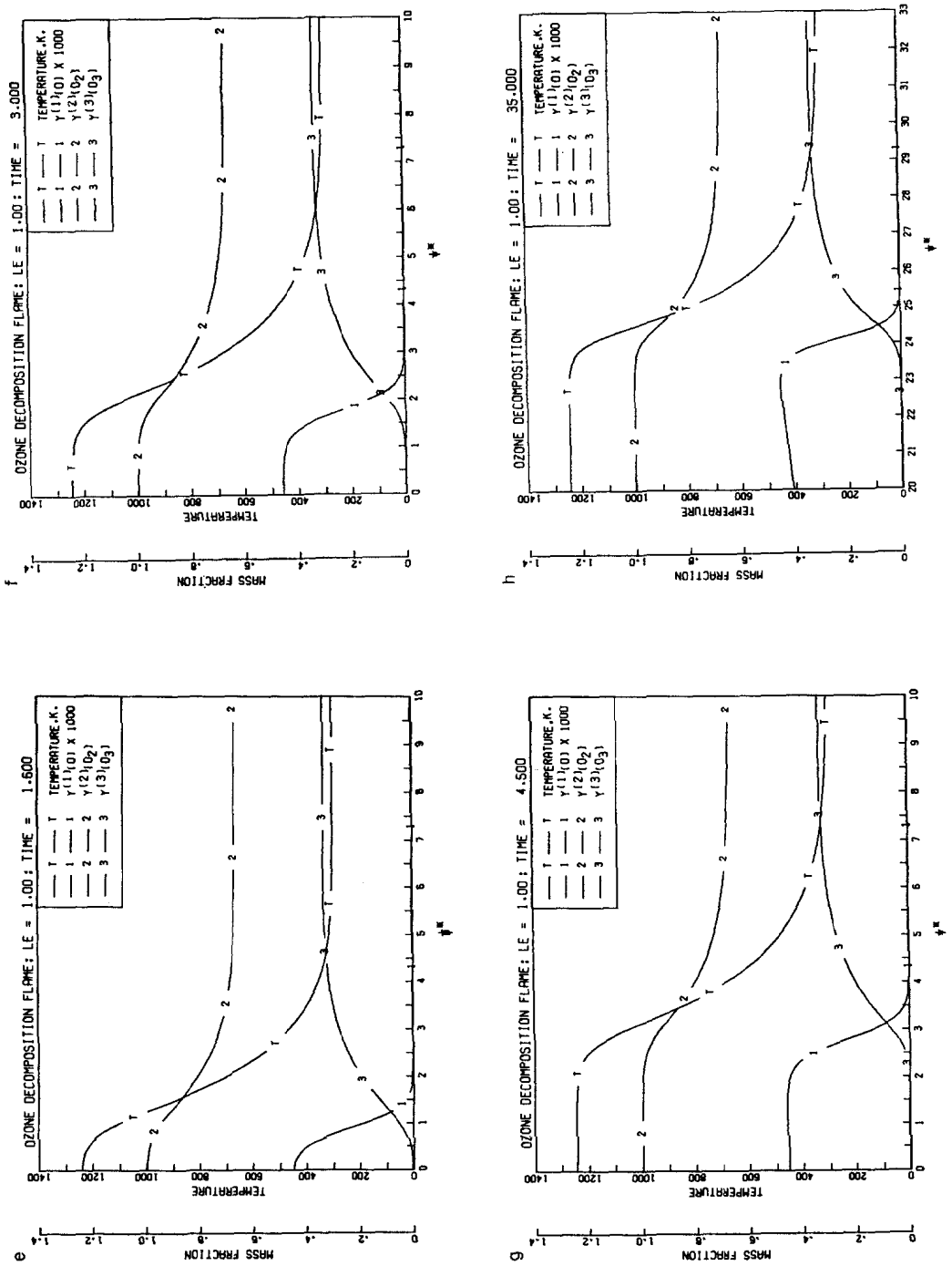


FIG. 2.—*Continued*

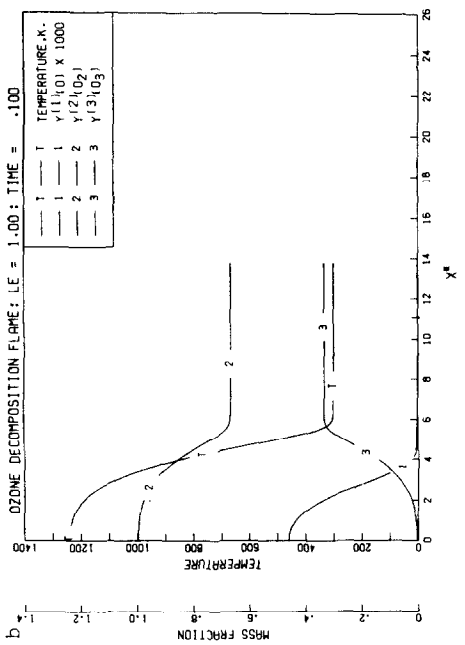
OZONE DECOMPOSITION FLAME: LE = 1.00; TIME = .100
T — T TEMPERATURE,K.
1 — 1 γ(1)(O) X 1000
2 — 2 γ(2)(O2)
3 — 3 γ(3)(O3)
TEMPERATURE
MASS FRACTION
χ*
b

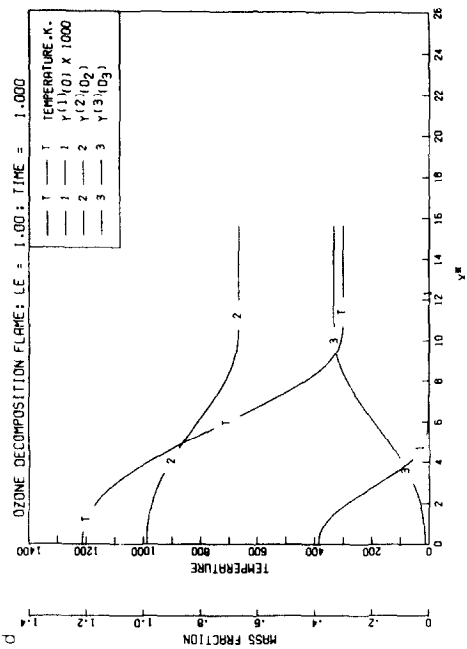
OZONE DECOMPOSITION FLAME: LE = 1.00; TIME = 1.000
T — T TEMPERATURE,K.
1 — 1 γ(1)(O) X 1000
2 — 2 γ(2)(O2)
3 — 3 γ(3)(O3)
TEMPERATURE
MASS FRACTION
χ*
d

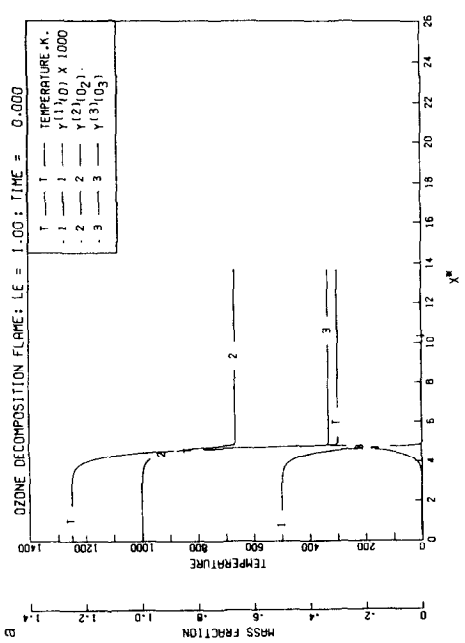
OZONE DECOMPOSITION FLAME: LE = 1.00; TIME = 0.000
T — T TEMPERATURE,K.
1 — 1 γ(1)(O) X 1000
2 — 2 γ(2)(O2)
3 — 3 γ(3)(O3)
TEMPERATURE
MASS FRACTION
χ*
a

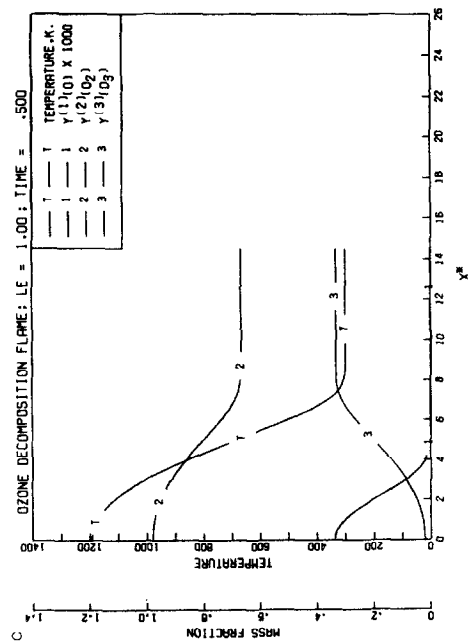
OZONE DECOMPOSITION FLAME: LE = 1.00; TIME = .500
T — T TEMPERATURE,K.
1 — 1 γ(1)(O) X 1000
2 — 2 γ(2)(O2)
3 — 3 γ(3)(O3)
TEMPERATURE
MASS FRACTION
χ*
c

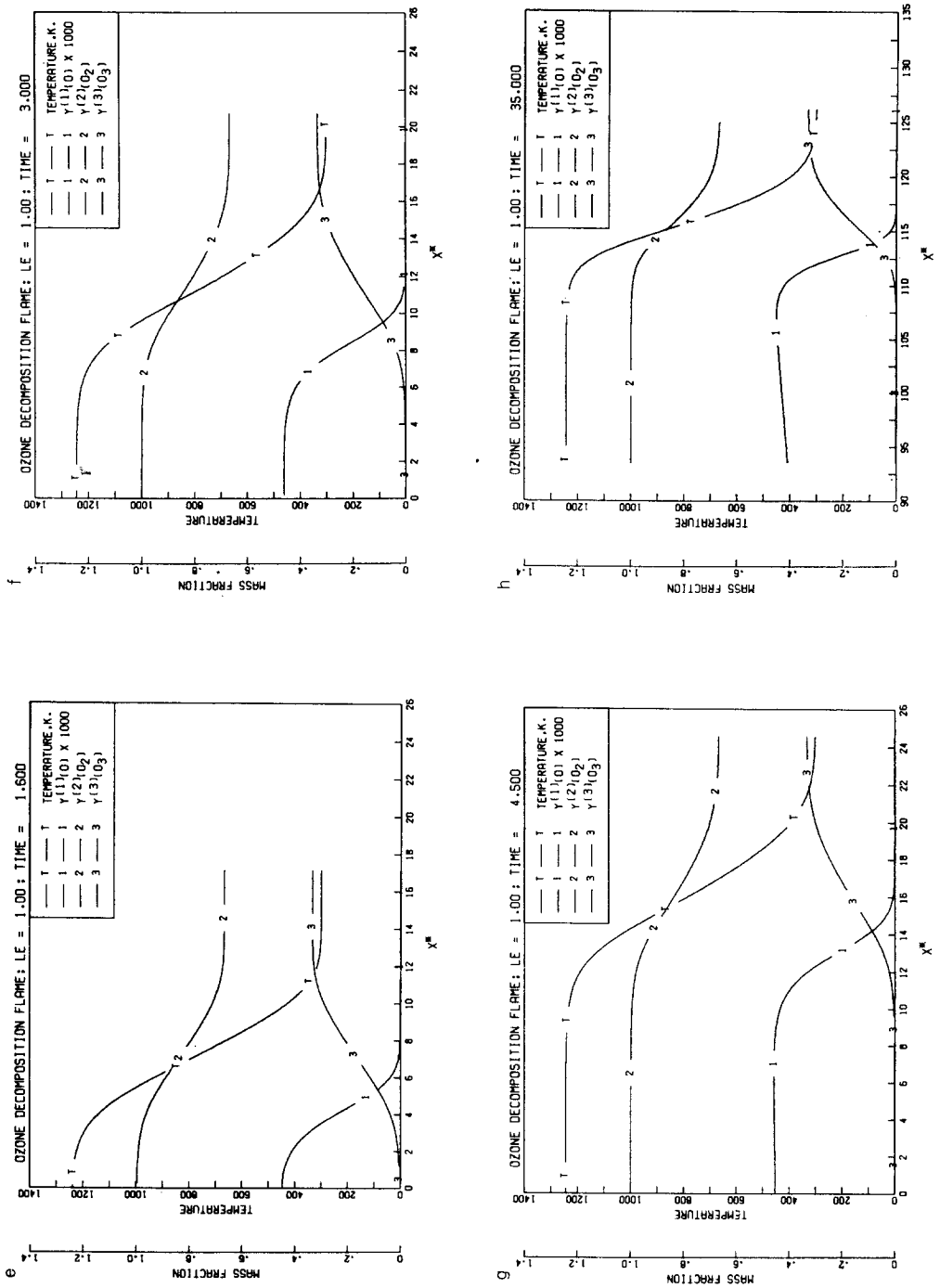


FIG. 3.—*Continued*

integral in Eq. (2.24), is shown in Fig. 4. At this stage, the velocity at infinity has essentially reached its constant value given by

$$u_\infty = \lim_{t\to\infty} u(x = \infty, t) = -\frac{1}{\rho_\infty}\int_0^\infty \frac{\partial\rho(\bar{x}, t)}{\partial t}\, d\bar{x}$$
$$= 184.6 \text{ cm/sec.} \tag{5.1}$$

The speed of propagation of the flame relative to the fluid at rest at the origin, $u_{f,0}$, was calculated (by measuring the distance travelled by the steady profile per unit time) to be 234.3 cm/sec, regardless of which profile was used to determine this

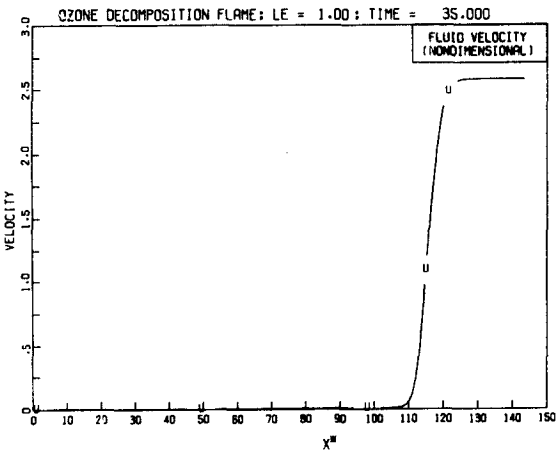


FIG. 4. Velocity profile through the quasi-steady ozone decomposition flame.

quantity. The flame speed $u_f$, the propagation velocity relative to the fluid at infinity, is thus

$$u_f = u_{f,0} - u_\infty = 49.7 \text{ cm/sec}, \tag{5.2}$$

as compared to Bledjian's value of about 54 cm/sec. Bledjian, however, reported variations in this value depending on which species was used to determine $u_{f,0}$ and hence was unable to truly obtain (in the limit $t^* \to \infty$) a flame which propagates without change in shape or velocity. Since this would imply that the steady-state eigenvalue problem referred to in Section 1 has no solution, the conclusion here is that high order methods such as the one demonstrated in this paper are essential to the theoretical prediction of time-dependent laminar flames.

## ACKNOWLEDGMENT

This research was supported by the Energy Research and Development Administration. The author would like to thank Drs. F. C. Gouldin, D. R. Hardesty, and R. E. Mitchell for several fruitful discussions during the course of this work.

## REFERENCES

1. J. O. HIRSCHFELDER, C. F. CURTISS, AND D. E. CAMPBELL, *J. Phys. Chem.* **57** (1953), 403.
2. F. A. WILLIAMS, "Combustion Theory," Addison–Wesley, Palo Alto, 1965.
3. K. A. WILDE, *Combust. Flame* **18** (1972), 43.
4. D. B. SPALDING, *Philos. Trans. Roy. Soc. London A* **249** (1956), 1.
5. D. B. SPALDING, P. L. STEPHENSON, AND R. G. TAYLOR, *Combust. Flame* **17** (1971), 55.
6. L. BLEDJIAN, *Combust. Flame* **20** (1973), 5.
7. N. K. MADSEN AND R. F. SINCOVEC, *in* "Numerical Methods for Differential Systems" (L. Lapidus and W. Schiesser, Eds.), pp. 229–242, Prentice–Hall, Englewood Cliffs, N.J., 1976.
8. H. B. CURRY AND I. J. SCHOENBERG, *J. Analyse Math.* **17** (1966), 71.
9. C. DE BOOR, *J. Approximation Theory* **6** (1972), 50.
10. C. DE BOOR, University of Wisconsin Math. Research Center Report 1333 (1973).
11. B. K. SWARTZ AND R. S. VARGA, *J. Approximation Theory* **6** (1972), 6.
12. N. K. MADSEN AND R. F. SINCOVEC, Lawrence Livermore Laboratory Preprint UCRL-78263 (1976); *ACM Trans.*, to appear.
13. A. C. HINDMARSH, Lawrence Livermore Laboratory Report UCID-30130 (1976).